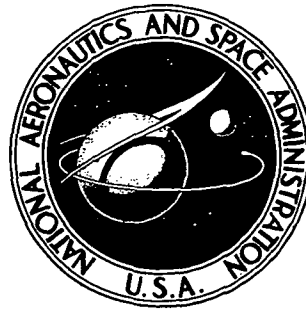


N72-32997

NASA TECHNICAL NOTE



NASA TN D-6994

NASA TN D-6994

**CASE FILE
COPY**

**APPLICATION OF THE LEADING-EDGE-SUCTION
ANALOGY TO PREDICTION OF LONGITUDINAL
LOAD DISTRIBUTION AND PITCHING MOMENTS
FOR SHARP-EDGED DELTA WINGS**

by Melvin H. Snyder, Jr., and John E. Lamar

Langley Research Center

Hampton, Va. 23365

NATIONAL AERONAUTICS AND SPACE ADMINISTRATION • WASHINGTON, D. C. • OCTOBER 1972

1. Report No. NASA TN D-6994	2. Government Accession No.	3. Recipient's Catalog No.	
4. Title and Subtitle APPLICATION OF THE LEADING-EDGE-SUCTION ANALOGY TO PREDICTION OF LONGITUDINAL LOAD DISTRIBUTION AND PITCHING MOMENTS FOR SHARP-EDGED DELTA WINGS		5. Report Date October 1972	
		6. Performing Organization Code	
7. Author(s) Melvin H. Snyder, Jr., Wichita State University; and John E. Lamar		8. Performing Organization Report No. L-8224	
		10. Work Unit No. 501-06-04-01	
9. Performing Organization Name and Address NASA Langley Research Center Hampton, Va. 23365		11. Contract or Grant No.	
		13. Type of Report and Period Covered Technical Note	
12. Sponsoring Agency Name and Address National Aeronautics and Space Administration Washington, D.C. 20546		14. Sponsoring Agency Code	
15. Supplementary Notes			
16. Abstract <p>The leading-edge-suction analogy of Polhamus has been used to develop the longitudinal load distribution of the vortex lift for delta wings. This distribution is shown to be similar in shape to that of the potential-flow longitudinal loading for delta wings having aspect ratios of 2 or less. The totals of the two theoretical distributions for delta wings with an aspect ratio near 1 are in good agreement with the experimentally determined loadings over the angle-of-attack range from 0° to 30°. The corresponding predicted pitching moments show slightly more stability than those measured, because of loss of lift near the wing tips.</p>			
17. Key Words (Suggested by Author(s)) Leading-edge vortex Longitudinal loading Delta wings Suction analogy		18. Distribution Statement Unclassified - Unlimited	
19. Security Classif. (of this report) Unclassified	20. Security Classif. (of this page) Unclassified	21. No. of Pages 20	22. Price* \$3.00

APPLICATION OF THE LEADING-EDGE-SUCTION ANALOGY TO PREDICTION OF LONGITUDINAL LOAD DISTRIBUTION AND PITCHING MOMENTS FOR SHARP-EDGED DELTA WINGS

By Melvin H. Snyder, Jr.,* and John E. Lamar
Langley Research Center

SUMMARY

The leading-edge-suction analogy of Polhamus has been used to develop the longitudinal load distribution of the vortex lift for delta wings. This distribution is shown to be similar in shape to that of the potential-flow longitudinal loading for delta wings having aspect ratios of 2 or less. The totals of the two theoretical distributions for delta wings with an aspect ratio near 1 are in good agreement with the experimentally determined loadings over the angle-of-attack range from 0° to 30° . The corresponding predicted pitching moments show slightly more stability than those measured, because of loss of lift near the wing tips.

INTRODUCTION

The nonlinear behavior of lift, drag, and pitching moment with angle of attack is of considerable interest because of its occurrence for the class of sharp-edged highly swept wings desirable for use in supersonic cruise vehicles and, possibly, in hypersonic vehicles. Many theoretical methods have been developed to predict the nonpotential, or vortex-lift, behavior (refs. 1 to 6). Most of these methods have limited applicability because of inherent assumptions, such as conical flow and slender wings (refs. 2 to 4), or because additional information is required to implement them (ref. 5). However, the leading-edge-suction analogy, originally postulated by Polhamus in reference 6 for the vortex lift on delta wings, has been shown to be a versatile technique which is useful over a broad range of planforms (refs. 6 to 8) and speeds (ref. 8). This analogy proposes that the low pressures associated with the leading-edge vortices produce a normal force which has the same magnitude as the potential-flow leading-edge-suction force that is lost because of the separation at the sharp leading edge. The suction analogy has been applied by Polhamus to predict the drag due to lift of delta wings (ref. 9) as well as arrow and diamond wings (ref. 7).

*Professor, Wichita State University.

Recently, Nangia and Hancock (ref. 10) concluded, from wind-tunnel tests at angles of attack at which the vortex lift was a significant portion of the total lift, that the longitudinal distribution of the vortex lift should be the same as for the potential lift on a slender delta wing. In order for this conclusion to be consistent with the leading-edge-suction analogy, the longitudinal distribution of the potential-flow leading-edge suction must be the same as the longitudinal distribution of the potential-flow lift. To evaluate their conclusion, the present study utilizes the vortex-lattice method of reference 11 to predict the distribution of the potential-flow leading-edge suction and then, by use of the Polhamus analogy, predicts the longitudinal distribution of vortex lift. The longitudinal distributions of the theoretical vortex lift and potential lift are compared and the total lift distribution is compared with experimental results. Ranges of aspect ratios and angles of attack were studied to determine limits of the validity of the Nangia and Hancock (ref. 10) conclusion.

SYMBOLS

A	aspect ratio, $\frac{b^2}{S_{\text{ref}}}$
b	wing span
b_l	local wing span, that is, the spanwise distance from one leading edge to the other at any chordwise position
c	local chord
\bar{c}	reference chord, $\frac{2}{3} c_r$
c_r	root chord
c_s	section suction-force coefficient, $\frac{1}{qc} \frac{dS}{dy}$
c_s'	station suction-force coefficient, $\frac{2}{qb_l} \frac{dS}{dx}$
C_L	lift coefficient, $\frac{\text{Lift}}{qS_{\text{ref}}}$
$C_{LL} = C_{NL} \cos \alpha$	
C_m	pitching-moment coefficient about $\frac{c_r}{2}$, $\frac{\text{Pitching moment}}{q\bar{c}S_{\text{ref}}}$

C_N	normal-force coefficient, $\frac{N}{qS_{\text{ref}}}$ (see eq. (7))
C_{NL}	longitudinal normal-loading coefficient, $C_{NL} = 2 \int_0^1 \left(\frac{x}{c_r}\right) \Delta C_p d\left(\frac{2y}{b_l}\right) = \frac{\partial N}{\partial x} \frac{b}{2}$
C_S	suction-force coefficient, $\frac{S}{qS_{\text{ref}}}$ (see eq. (12))
C_{SL}	longitudinal suction-force coefficient, $c_s(c/c_r)$
ΔC_p	pressure-difference coefficient, $\frac{p_{\text{lower}} - p_{\text{upper}}}{q}$
K_p, K_v	coefficients used in Polhamus' suction analogy (see eqs. (2) and (3))
N	normal force
p	static pressure
q	free-stream dynamic pressure
S	suction force
S_{ref}	reference area, $\frac{bc_r}{2}$
V	free-stream velocity
x	chordwise coordinate in wing plane, origin at apex and positive aft (see fig. 1(b))
y	spanwise coordinate, origin at center line and positive toward right wing tip (see fig. 1(b))
α	angle of attack, deg
Subscripts:	
p	potential flow
v	vortex flow

DISCUSSION AND RESULTS

Vortex-Lift Theory

From flight and wind-tunnel studies, the flow around wings having sharp leading edges has been observed to separate at all but the very lowest angles of attack. For wings having leading-edge sweepback, this separated flow rolls up into basically two helical vortices, the cores of which are inboard of the leading edges and above the wing-chord plane. As shown in figure 1(a), the flow reattaches inboard of the vortices. Data indicate that when leading-edge separation occurs, the wing lift generated exceeds that predicted by potential-flow solutions. Some authors have postulated that the total lift could be thought of as being composed of the potential-flow lift and a lift term associated with the vortex flow, that is, $C_L = C_{L,p} + C_{L,v}$.

The vortex-flow lift expression developed in reference 6 employs this postulate and is based on the concept that the leading-edge suction force, which exists in attached flow, is rotated into a normal force when the leading-edge flow separates. This concept led to

$$C_L = \overbrace{K_p \sin \alpha \cos^2 \alpha}^{C_{L,p}} + \overbrace{K_v \sin^2 \alpha \cos \alpha}^{C_{L,v}} \quad (1)$$

where

$$K_p = \frac{\partial C_{N,p}}{\partial (\sin \alpha \cos \alpha)} \quad (2)$$

$$K_v = \frac{\partial C_s}{\partial (\sin^2 \alpha)} \quad (3)$$

and K_p and K_v depend only on planform and Mach number. Comparisons of Polhamus' expression with experiment presented in references 6, 8, 12, and 13 show good agreement over the range of α , including the cases in which a large proportion of the total lift comes from the vortex flow. Extensive experimental data were available from reference 14 for the $A = 1.147$ flat delta wing which was used in the present study for comparison with the calculated lift curves. Figure 2 shows the excellent agreement of these data with the predicted values from equation (1).

Longitudinal Lift Distribution

For slender wings, it is useful to consider the load distribution in the longitudinal direction. This force distribution has been termed variously: chordwise (refs. 10, 15,

and 16); stream (ref. 10), longitudinal (ref. 10), lengthwise (ref. 10), and cross-load (ref. 17) distribution. In this paper, this loading is termed longitudinal loading in contradistinction to chordwise loading, which will be reserved for a given spanwise position.

The longitudinal loadings used in this paper are determined by the procedures outlined by Nangia and Hancock (ref. 10) and detailed here. Normally, N is determined from wing pressure data by the expression

$$N = q \frac{b}{2} \int_{-1}^1 c \int_{le}^{te} \Delta C_p dx d\left(\frac{2y}{b}\right) \quad (4)$$

where le and te refer to the leading and trailing edge, respectively. However, it can alternately be expressed as

$$N = qc_r \int_0^1 \frac{b_l}{2} \int_{-1}^1 \Delta C_p d\left(\frac{2y}{b_l}\right) d\left(\frac{x}{c_r}\right) \quad (5)$$

From the geometric relationships which exist on a delta wing, it is known that

$$\frac{b_l}{b} = \frac{x}{c_r} \quad (6)$$

Hence, by combining the preceding equations, the results can be written in coefficient form as

$$C_N = \int_0^1 C_{NL} d\left(\frac{x}{c_r}\right) \quad (7)$$

where

$$C_{NL} = 2 \int_0^1 \left(\frac{x}{c_r}\right) \Delta C_p d\left(\frac{2y}{b_l}\right) = \frac{\partial N}{\partial x} \frac{b}{q \frac{b}{2}} \quad (8)$$

The vortex-lift longitudinal loading, however, is obtained by a different procedure. This difference is due to the unique character of the vortex lift in that, rather than being the result of distributed pressure over an area, it is better regarded as a force per length distributed along each of the leading edges. The magnitude of this force is the same as that of the leading-edge suction force – the distribution of which can be determined by many computer programs based on lifting-surface theory. The vortex-lattice computer program of reference 11 was employed to provide the suction distributions used herein. The lattice arrangement selected for representing the delta wings in this study consisted of 10 chordwise positions at each of 12 spanwise stations on a half-wing, as shown in

figure 1(b). This choice of vortex lattice was the result of a systematic study of the effects of varying the number of chordwise and spanwise stations (with the maximum number of vortices limited to 120). Two criteria were used, the first being comparison of the calculated value of K_v with that cited in reference 6. The second criterion was that the normalized C_{SL} curve must not have negative values and should go to zero, with the slope approaching infinity at the apex, as indicated by reference 18.

It is conventional to express the leading-edge suction force in terms of a section coefficient c_s defined by

$$\frac{S}{2} = \int_0^{b/2} c_s c_q dy = \int_0^1 c_s \frac{b}{2} c_q d\left(\frac{y}{b/2}\right) \quad (9)$$

This section suction-force coefficient is provided by the vortex-lattice program as a function of $\frac{y}{b/2}$. The suction force may also be expressed in terms of a station suction coefficient c'_s :

$$\frac{S}{2} = \int_0^{c_r} c'_s q \frac{b_l}{2} dx = \int_0^1 c'_s c_r \frac{b_l}{2} q d\left(\frac{x}{c_r}\right) \quad (10)$$

Because of the delta planform, $\frac{x}{c_r} = \frac{y}{b/2}$. Equations (9) and (10) may be combined to relate the two coefficients:

$$c'_s c_r b_l = c_s c b \quad (11)$$

In order to compare the vortex-lift longitudinal loading with the potential-lift longitudinal loading, it is desirable to use the same form as equation (7):

$$C_S = 2 \int_0^1 C_{SL} d\left(\frac{x}{c_r}\right) \quad (12)$$

and

$$S = C_S q S_{ref} \quad (13)$$

Equations (9) to (13) lead to the equation used to obtain C_{SL} from the computer program:

$$C_{SL} = c_s \left(1 - \frac{x}{c_r}\right) = c_s \left(\frac{c}{c_r}\right) \quad (14)$$

The results are presented in terms of $\frac{2C_{SL}}{C_S}$ which by use of the suction analogy is equivalent to $\left(\frac{C_{NL}}{C_N}\right)_v$ and, consequently, to $\left(\frac{C_{LL}}{C_L}\right)_v$. The longitudinal vortex-loading coefficient as defined by equations (12) and (14) is consistent with the previously defined potential loading.

In reference 10, Nangia and Hancock reported the results of a series of wind-tunnel tests conducted on flat and cambered sharp-edged delta-wing models of $A = 1$. With the use of experimental pressure data $\frac{C_{LL}}{C_L}$, which is equivalent to $\frac{C_{NL}}{C_N}$, was obtained by evaluation of equation (8). The longitudinal loading was compared with a similar distribution predicted by the subsonic lifting-surface theory of Taylor (ref. 16). Since the normalized curve of potential-lift longitudinal loading was very similar to the normalized curve of total lift, Nangia and Hancock concluded that the variation of vortex lift must also have the same shape.

The present report is concerned with this conclusion. To determine its validity limits, a systematic study of the longitudinal-loading characteristics of flat delta wings was performed by using the vortex-lattice program of reference 11. The normalized potential-lift and vortex-lift curves obtained with this program for an $A = 1$ delta wing are compared with data from Nangia and Hancock (ref. 10) in figure 3. Figure 4 shows the potential-lift and vortex-lift longitudinal loadings for an $A = 1.147$ wing compared with data reported in reference 14. Both figures 3 and 4 indicate general agreement in the forms of the vortex-lift and potential-lift curves and close agreement with the experimental data for total lift. The experimental data show some slight variation in the shape of the longitudinal loadings with angle of attack, whereas the theoretical loadings are independent of α .

Effects of Angle of Attack and Aspect Ratio

In addition to the changes in the forms of the normalized longitudinal-loading variation with angle of attack, a second angle-of-attack effect is shown in figure 5. An examination of this figure shows that the potential- and vortex-lift longitudinal loadings change proportions with α in such a way that a theoretical total is produced which, in general, agrees in shape with the experimental distribution even though the two curves have slightly different centroids. Note, in particular, the more rapid growth of the vortex-lift longitudinal loading with α than that for the potential lift – a characteristic of the lift development in this separated flow regime.

The variations of the potential- and vortex-lift longitudinal loadings with aspect ratio are presented in figure 6. The most interesting feature noted in a comparison of the two sets of curves ((a) and (b) parts) is that as the aspect ratio decreases, the two kinds of

loadings approach one another. In fact, it is easy to show from slender-wing theory that the loadings are identical in the limit as $A \rightarrow 0$. However, as the aspect ratio is increased above say 2, the similarity in shape of the two loadings no longer exists. Thus, the conclusion of reference 10 holds only over a limited range of aspect ratio.

Figure 6 also shows that the variation of longitudinal loading with aspect ratio is greater for the vortex lift than for the potential lift. This occurs because the vortex-lift distribution is obtained from the leading-edge-suction distribution, which is really associated with a point on the leading edge rather than along either the span or the root chord. Hence, it may be graphed for a delta wing in either normalized coordinate direction without changing the shape. The reason for this behavior is that the leading-edge suction exists at the leading edge and is not distributed along the chord or span, even though it is dependent upon the negative pressure rise along a normal to the edge. With delta wings of small aspect ratio, normal to the leading edge is almost the same as normal to the root chord. Hence, graphing the vortex-lift loading along the root chord is appropriate. However, as the aspect ratio increases to some value ($A = 16$ illustrated in fig. 6) for which the sweepback angle becomes low, then the normal direction to the leading edge is nearly normal to the span (rather than to the chord), and hence, graphing the loading along the root chord is not appropriate. In fact, for the $A = 16$ delta wing, the vortex-lift loading resembles a span load distribution more than it does the potential-lift longitudinal loading.

Pitching-Moment Prediction

The pitching-moment coefficient for the potential and vortex lift can be predicted by using the appropriate longitudinal loadings in the following equation:

$$(C_m)_{p,v} = \frac{3}{2} \left[\frac{C_N}{2} - \int_0^1 \frac{x}{c_r} C_{NL} d\left(\frac{x}{c_r}\right) \right]_{p,v}$$

The results of computations made with this equation are shown in figure 7 as a function of α . From the figure, it is seen that the vortex lift produces a stabilizing moment and becomes the larger contributor at the high angles of attack. The sum of these curves is compared in figure 8 with the experimental data of reference 17 ($A = 1.0$) and in figure 9 with the experimental data of references 13 and 14 ($A = 1.147$). In each case, the theory predicts a nose-down moment of larger magnitude than is obtained from experiment. The difference is in the direction expected to be caused by the actual loading centroid being forward of the theoretical — caused by loss of lift near the model wing tips. The theoretical curve predicted in reference 13 by use of the computer program described in reference 19 coincides with the present prediction in figure 9.

CONCLUDING REMARKS

The leading-edge-suction analogy of Polhamus is used to develop the vortex-lift longitudinal load distribution for delta wings. This type of loading has been combined with that obtained from potential-flow concepts and the combination has been compared with that determined experimentally. Good agreement has been determined for delta wings with aspect ratios of 1.0 and 1.147 at several different angles of attack.

The Nangia and Hancock conclusion (in C.P. No. 1129, Brit. A.R.C.) that similar longitudinal load distributions result for vortex-flow and potential-flow lifts has been verified by the suction analogy for delta wings with aspect ratios of 2 or less.

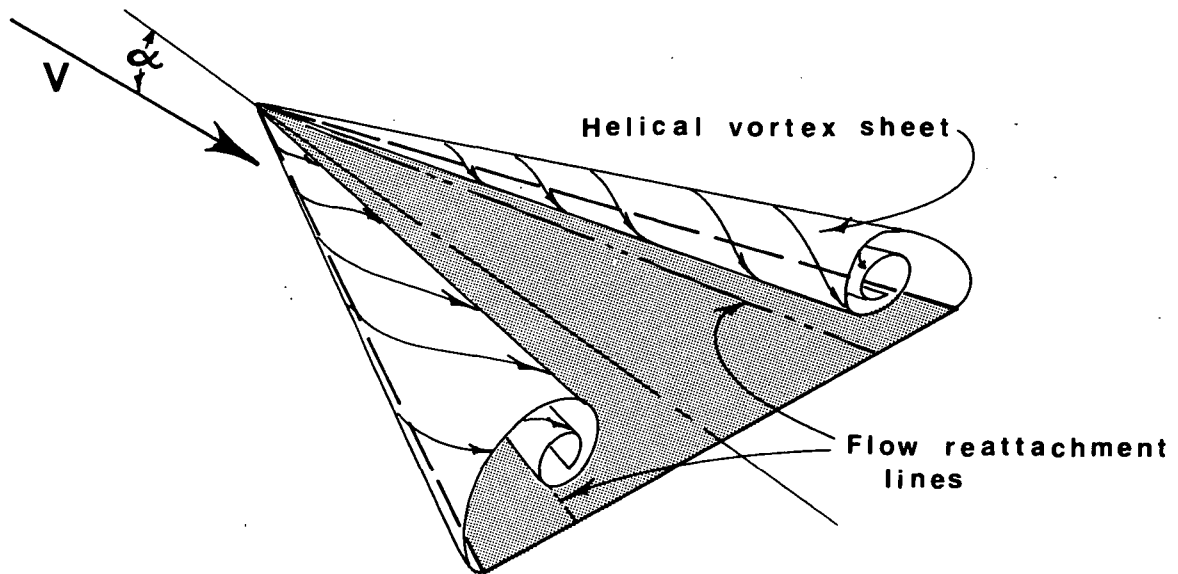
The theoretical longitudinal load distributions have also been used to predict the nonlinear pitching-moment behavior of delta wings. A comparison with experiment shows that the theory predicts slightly greater stability than measured.

Langley Research Center,
National Aeronautics and Space Administration,
Hampton, Va., September 20, 1972.

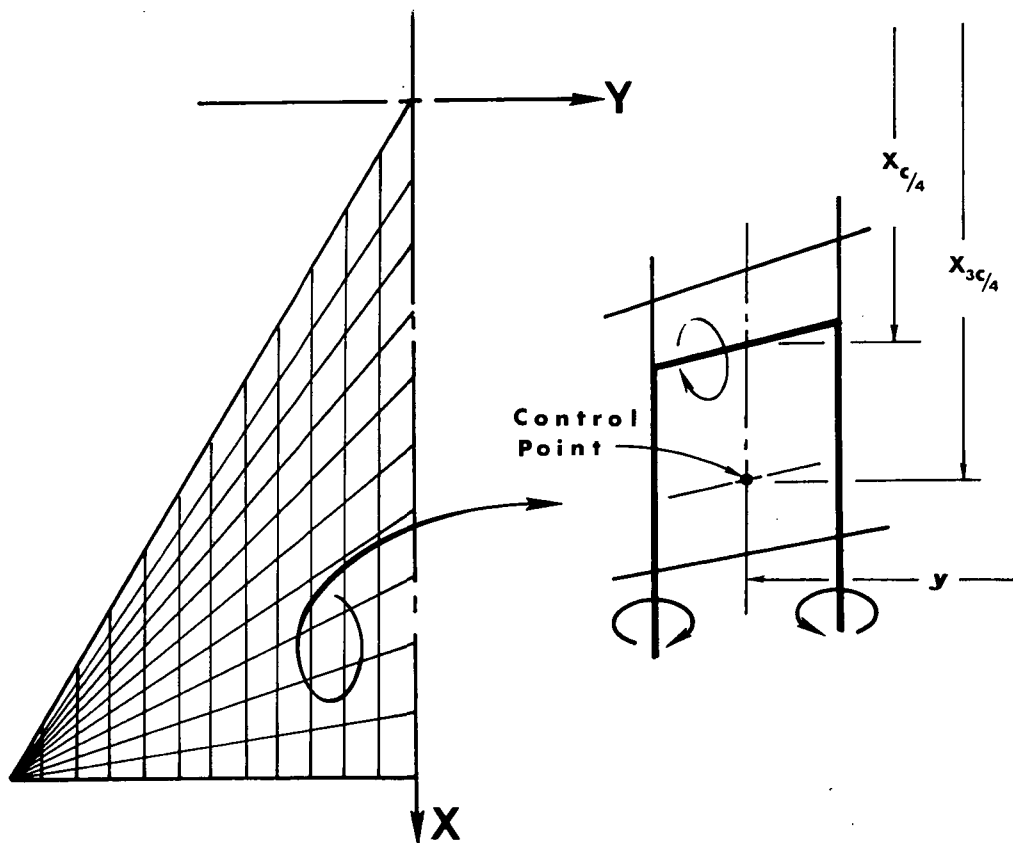
REFERENCES

1. Gersten, K.: Calculation of Non-Linear Aerodynamic Stability Derivatives of Aeroplanes. AGARD Rep. 342, Apr. 1961.
2. Brown, Clinton E.; and Michael, William H., Jr.: On Slender Delta Wings With Leading-Edge Separation. NACA TN 3430, 1955.
3. Mangler, K. W.; and Smith, J. H. B.: A Theory of the Flow Past a Slender Delta Wing With Leading Edge Separation. Proc. Roy. Soc. (London), ser. A, vol. 251, May 26, 1959, pp. 200-217.
4. Nangia, R. K.; and Hancock, G. J.: A Theoretical Investigation for Delta Wings With Leading-Edge Separation at Low Speeds. C.P. No. 1086, Brit. A.R.C., 1970.
5. Sacks, Alvin H.; Lundberg, Raymond E.; and Hanson, Charles W.: A Theoretical Investigation of the Aerodynamics of Slender Wing-Body Combinations Exhibiting Leading-Edge Separation. NASA CR-719, 1967.
6. Polhamus, Edward C.: A Concept of the Vortex Lift of Sharp-Edge Delta Wings Based on a Leading-Edge-Suction Analogy. NASA TN D-3767, 1966.
7. Polhamus, Edward C.: Charts for Predicting the Subsonic Vortex-Lift Characteristics of Arrow, Delta, and Diamond Wings. NASA TN D-6243, 1971.
8. Polhamus, Edward C.: Predictions of Vortex-Lift Characteristics by a Leading-Edge Suction Analogy. J. Aircraft, vol. 8, no. 4, Apr. 1971, pp. 193-199.
9. Polhamus, Edward C.: Application of the Leading-Edge-Suction Analogy of Vortex Lift to the Drag Due to Lift of Sharp-Edge Delta Wings. NASA TN D-4739, 1968.
10. Nangia, R. K.; and Hancock, G. J.: Delta Wings With Longitudinal Camber at Low Speed. C.P. No. 1129, Brit. A.R.C., 1970.
11. Margason, Richard J.; and Lamar, John E.: Vortex-Lattice FORTRAN Program for Estimating Subsonic Aerodynamic Characteristics of Complex Planforms. NASA TN D-6142, 1971.
12. Wentz, William H., Jr.; and Kohlman, David L.: Wind-Tunnel Investigations of Vortex Breakdown on Slender Sharp-Edged Wings. Rep. FRL 68-013 (Grant NGR-17-002-043), Univ. of Kansas, Center for Res., Inc., Nov. 27, 1968. (Available as NASA CR-98737.)
13. Davenport, Edwin E.; and Huffman, Jarrett K.: Experimental and Analytical Investigation of Subsonic Longitudinal and Lateral Aerodynamic Characteristics of Slender Sharp-Edge 74° Swept Wings. NASA TN D-6344, 1971.

14. Wentz, W. H., Jr.: Effects of Leading-Edge Camber on Low-Speed Characteristics of Slender Delta Wings. NASA CR-2002, 1972.
15. Kirkpatrick, D. L. I.: Analysis of the Static Pressure Distribution on a Delta Wing in Subsonic Flow. R. & M. No. 3619, Brit. A.R.C., 1970.
16. Taylor, C. R.: A Subsonic Lifting-Surface Theory for Low Aspect-Ratio Wings. R. & M. No. 3051, Brit. A.R.C., 1957.
17. Peckham, D. H.: Low-Speed Wind-Tunnel Tests of a Series of Uncambered Slender Pointed Wings With Sharp Edges. R. & M. No. 3186, Brit. A.R.C., 1961.
18. Rossiter, Patricia J.: The Linearized Subsonic Flow over the Centre-Section of a Lifting Swept Wing. R. & M. No. 3630, Brit. A.R.C., 1970.
19. Wagner, Siegfried: On the Singularity Method of Subsonic Lifting-Surface Theory. AIAA Paper No. 69-37, Jan. 1969.



(a) Leading-edge separation vortices.



(b) Vortex-lattice representation.

Figure 1.- Separated and attached flow-field representations for the delta wing.

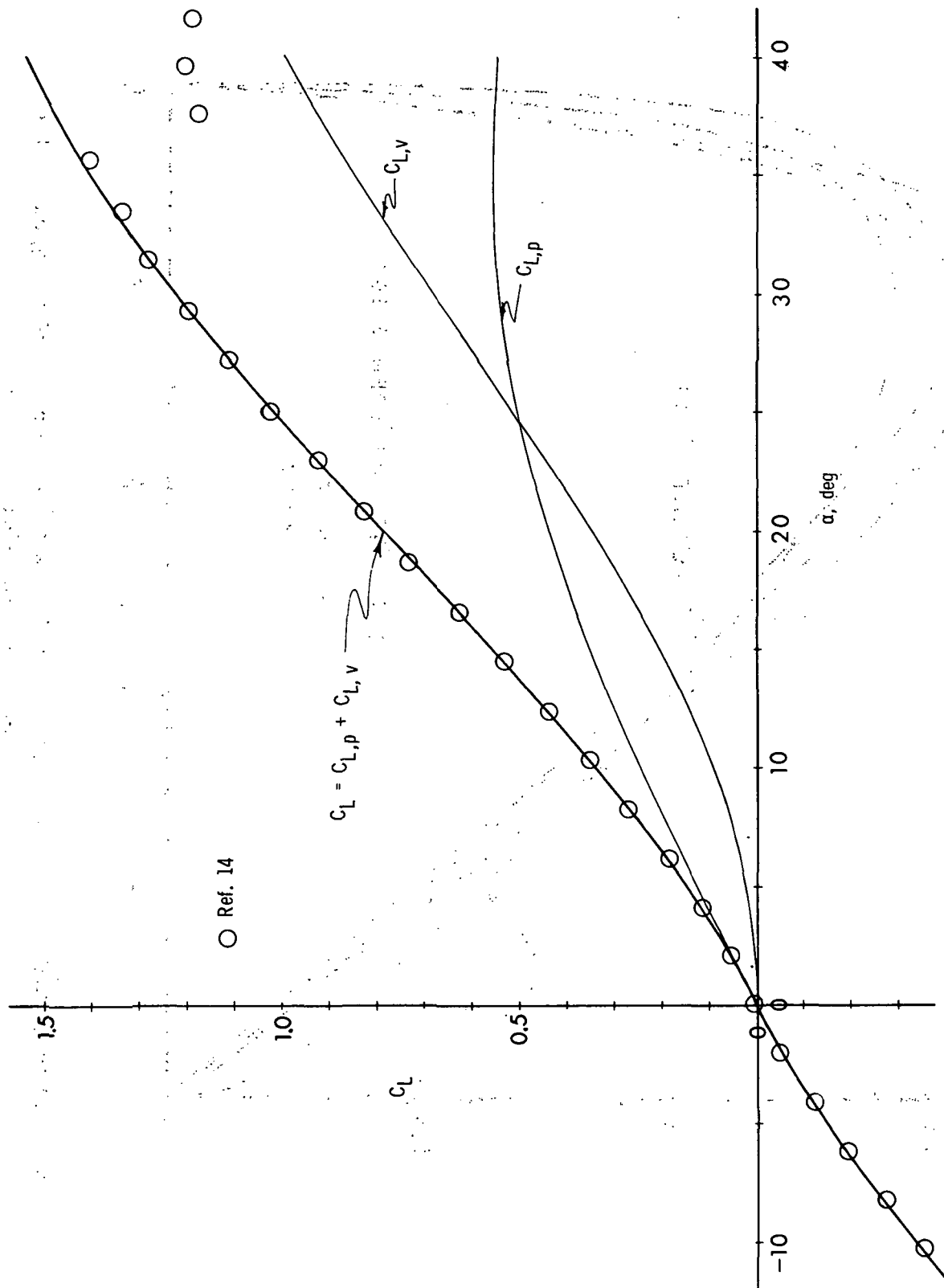


Figure 2.- Variation of C_L as measured and predicted for an $A = 1.147$ delta wing.

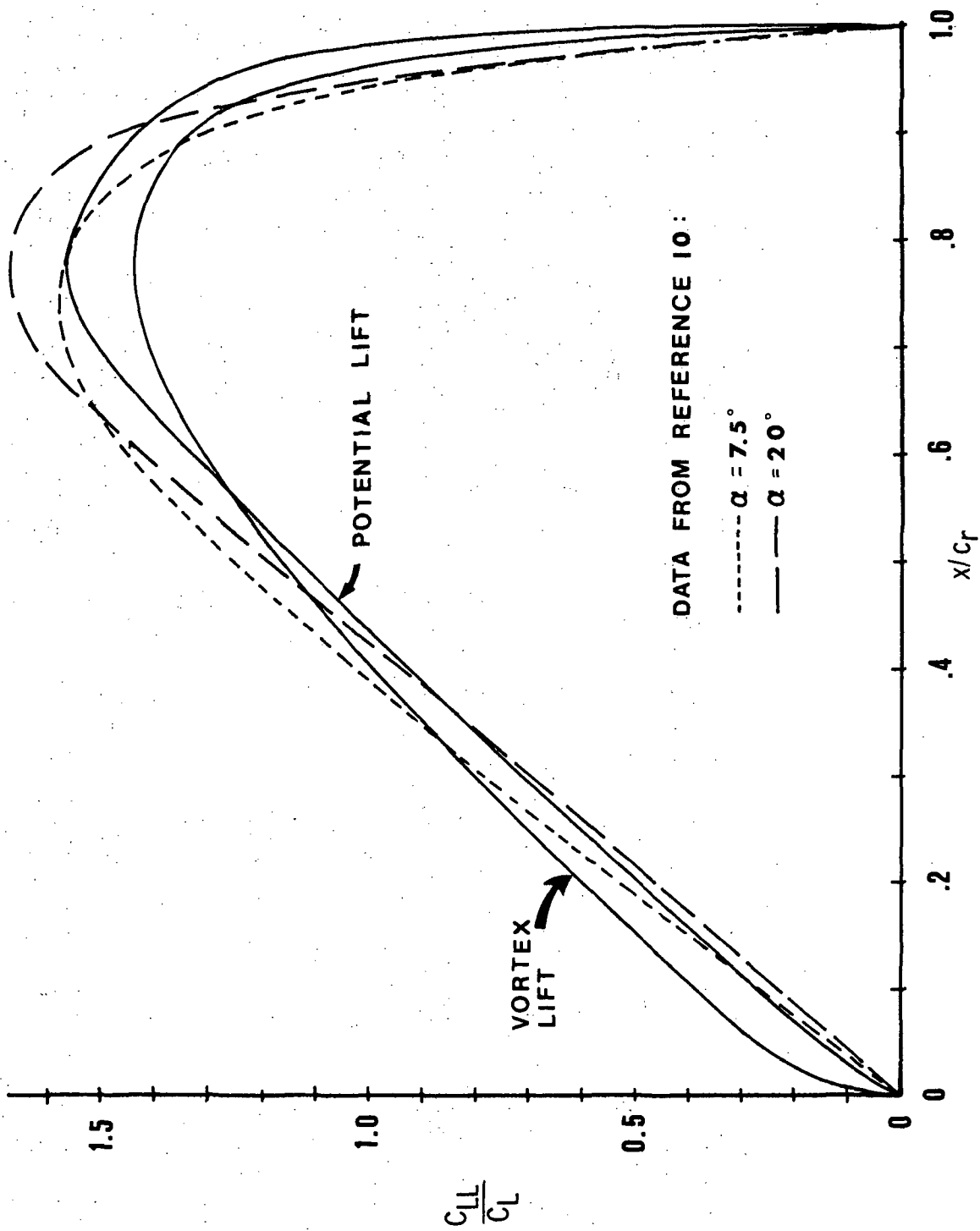


Figure 3.- Effect of angle of attack on the theoretical and experimental normalized longitudinal loadings for an $A = 1$ delta wing.

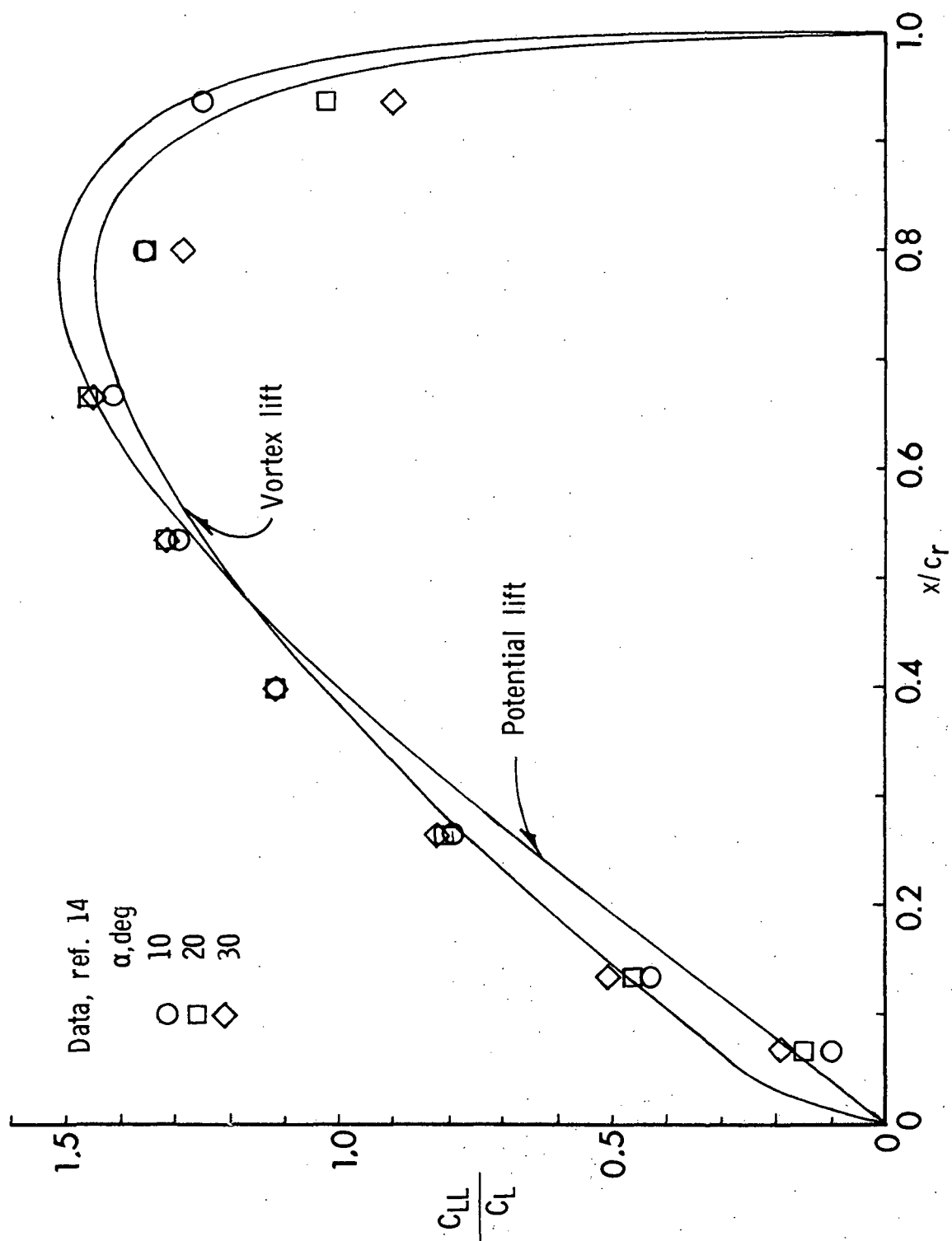


Figure 4.- Effect of angle of attack on the theoretical and experimental normalized longitudinal loadings for an $A = 1.147$ delta wing.

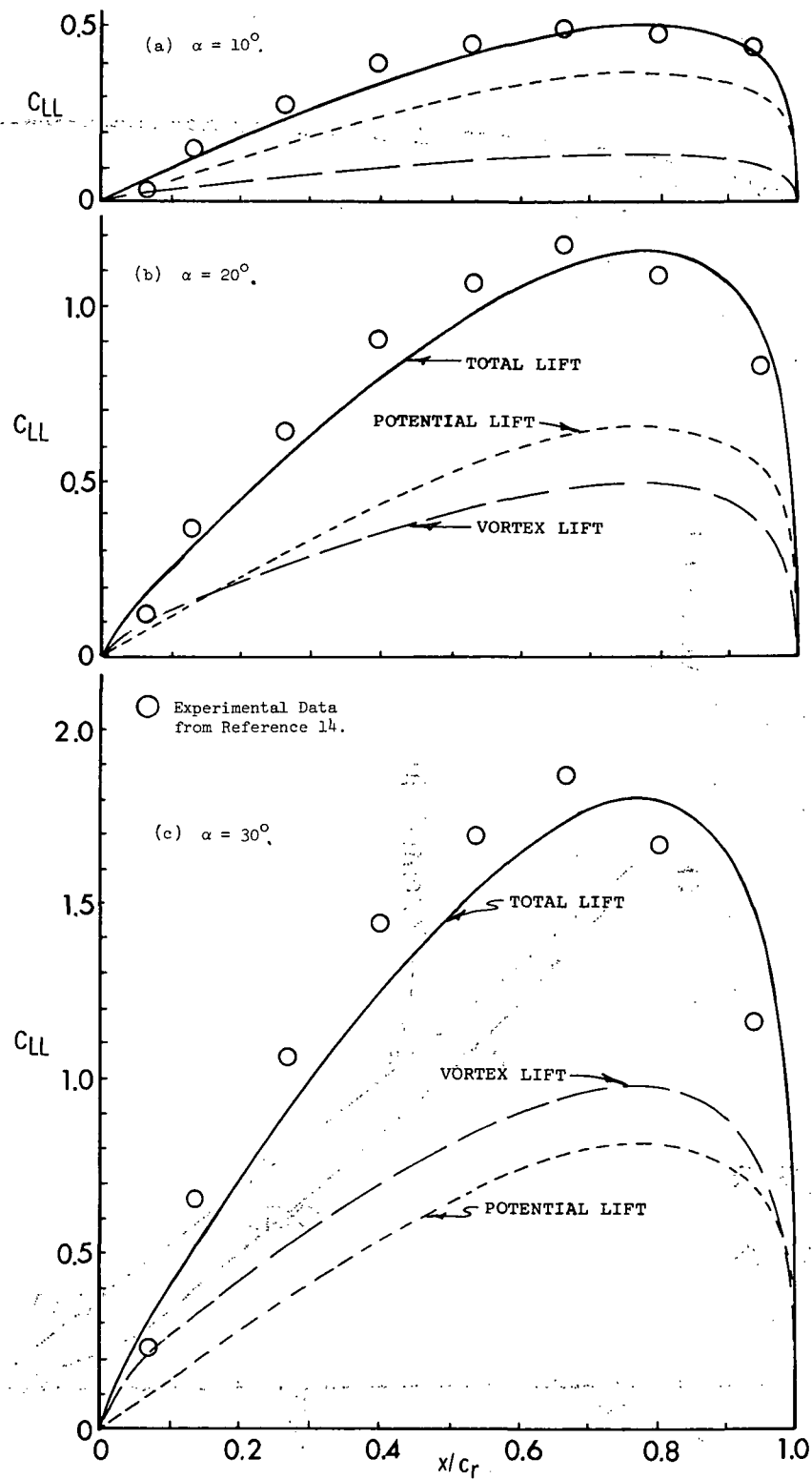
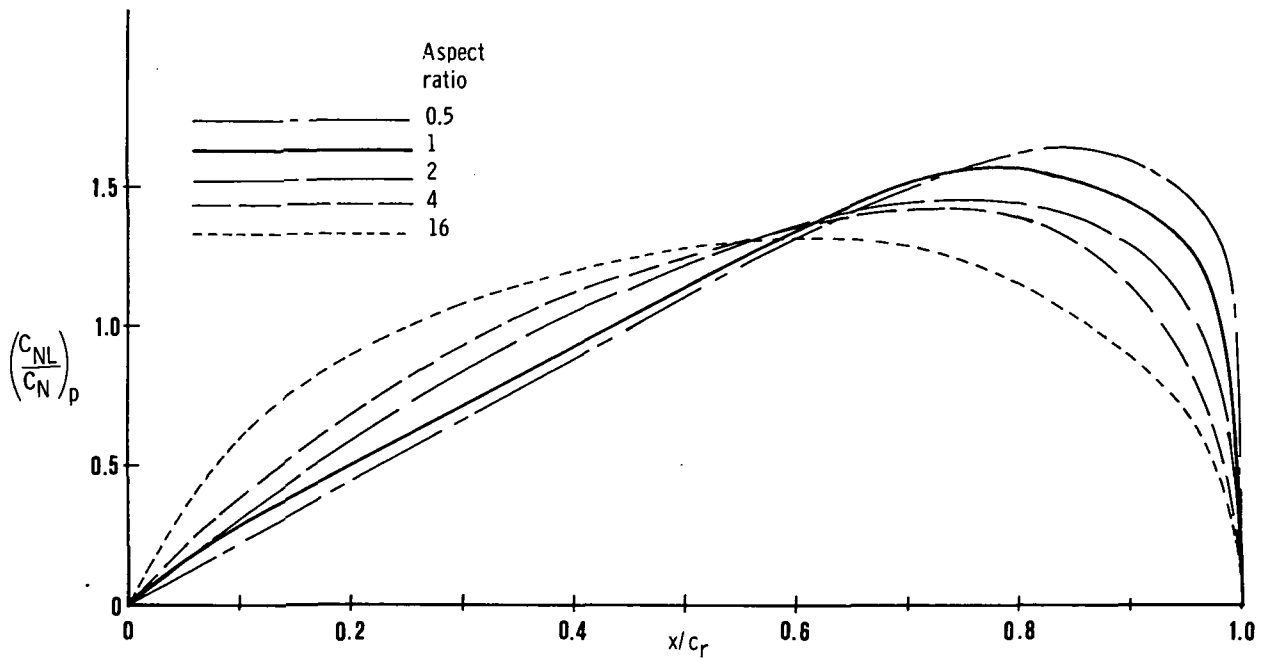
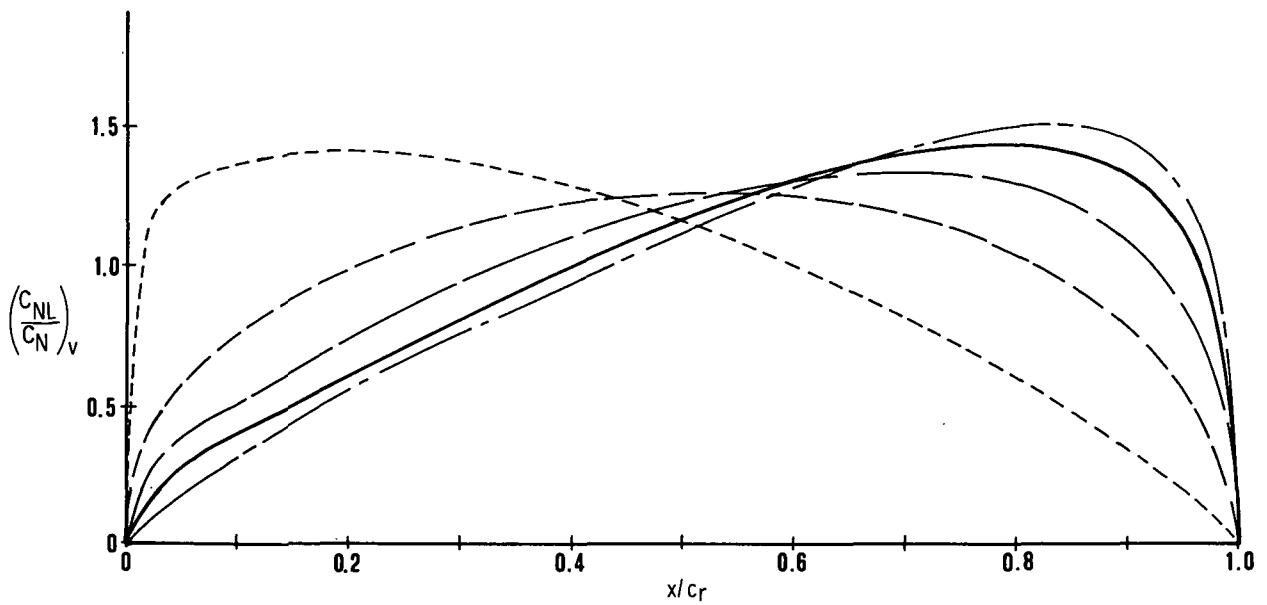


Figure 5.- Combinations of the vortex- and potential-lift longitudinal loadings along with the experimental loadings at several angles of attack for an $A = 1.147$ delta wing.



(a) Potential-lift loading.



(b) Vortex-lift loading.

Figure 6.- Effect of aspect ratio on the normalized longitudinal loadings.

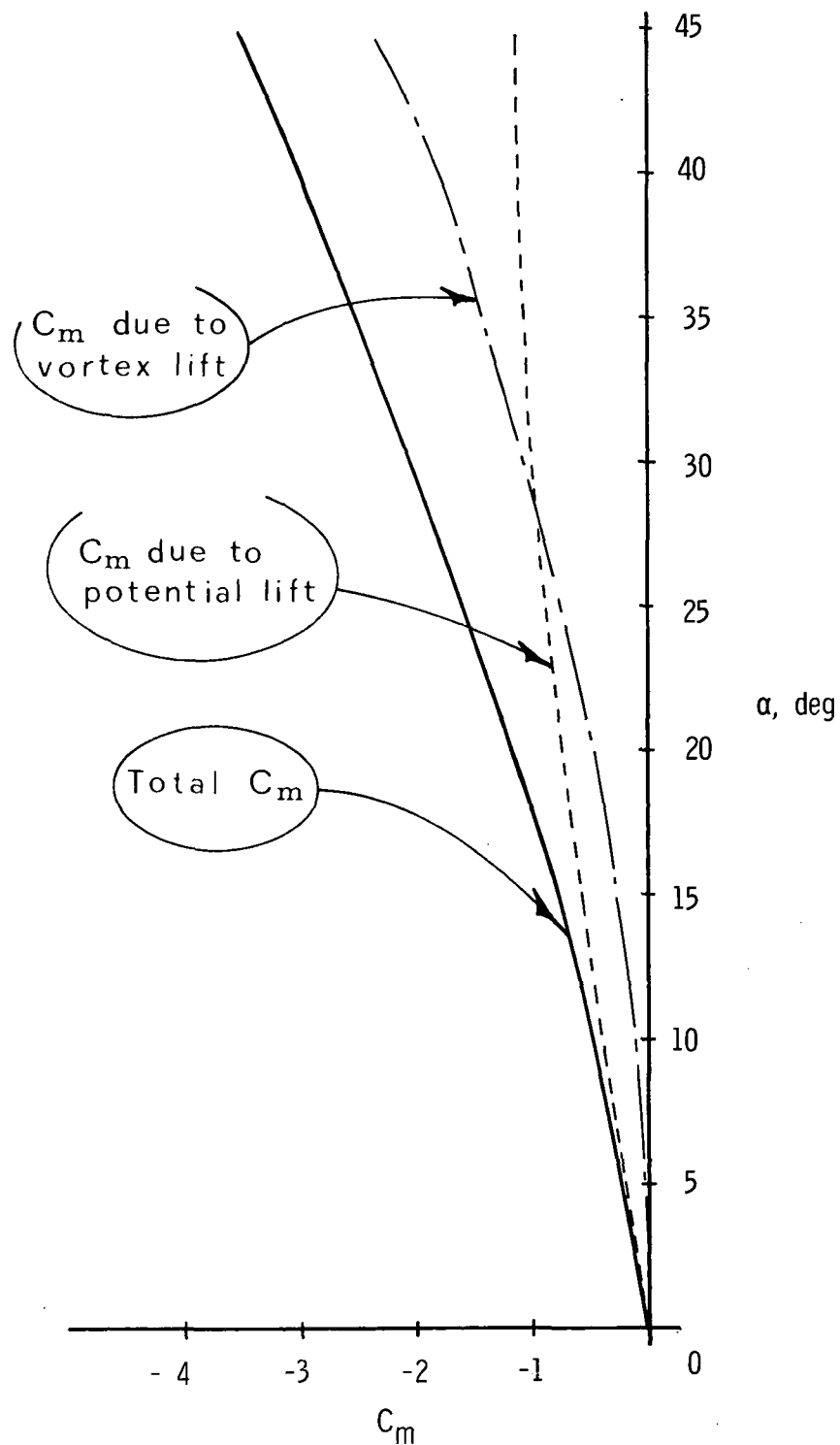


Figure 7.- Combinations of pitching-moment contributions from the potential- and vortex-lift longitudinal loadings at various angles of attack for an $A = 1$ delta wing.

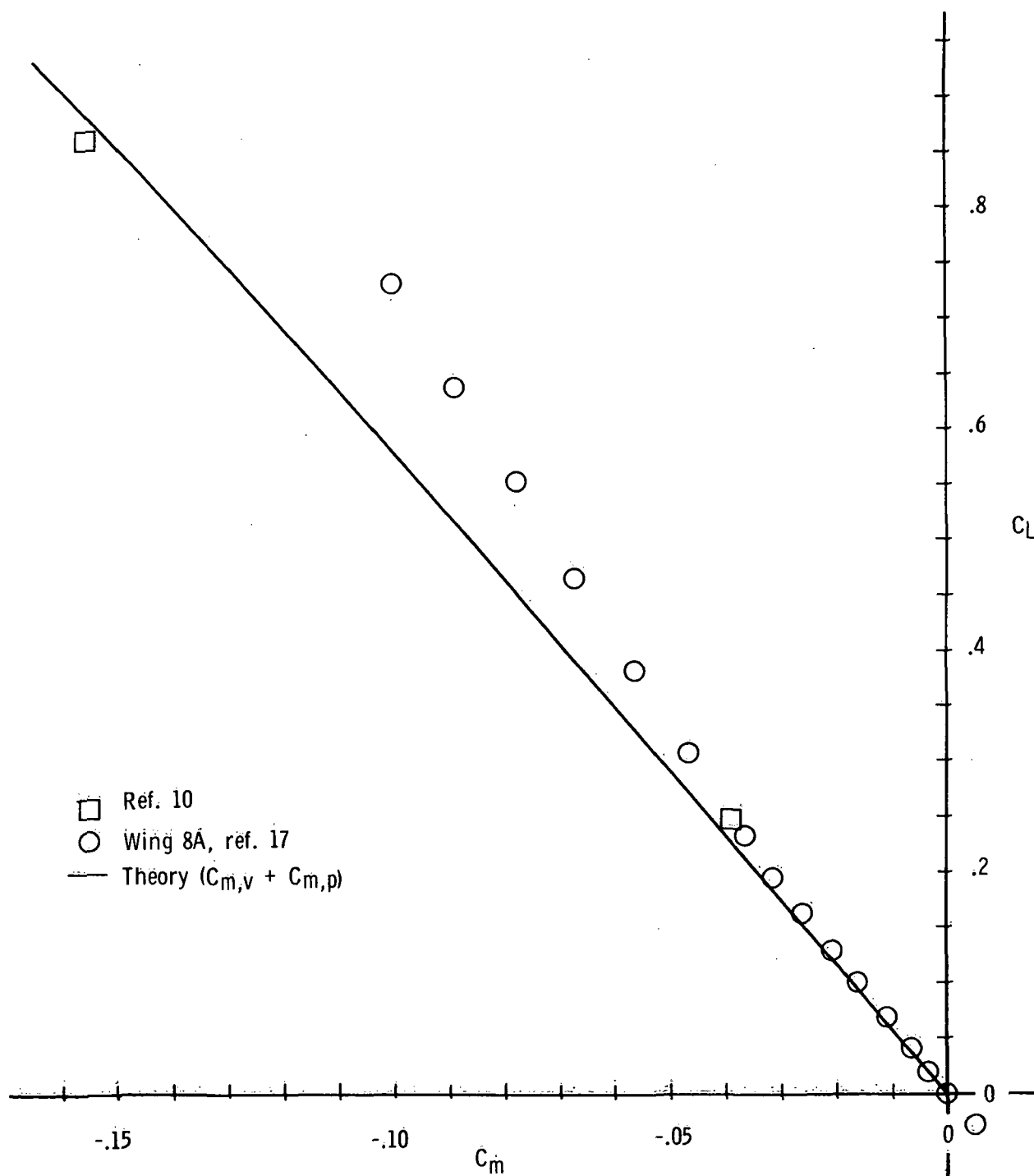
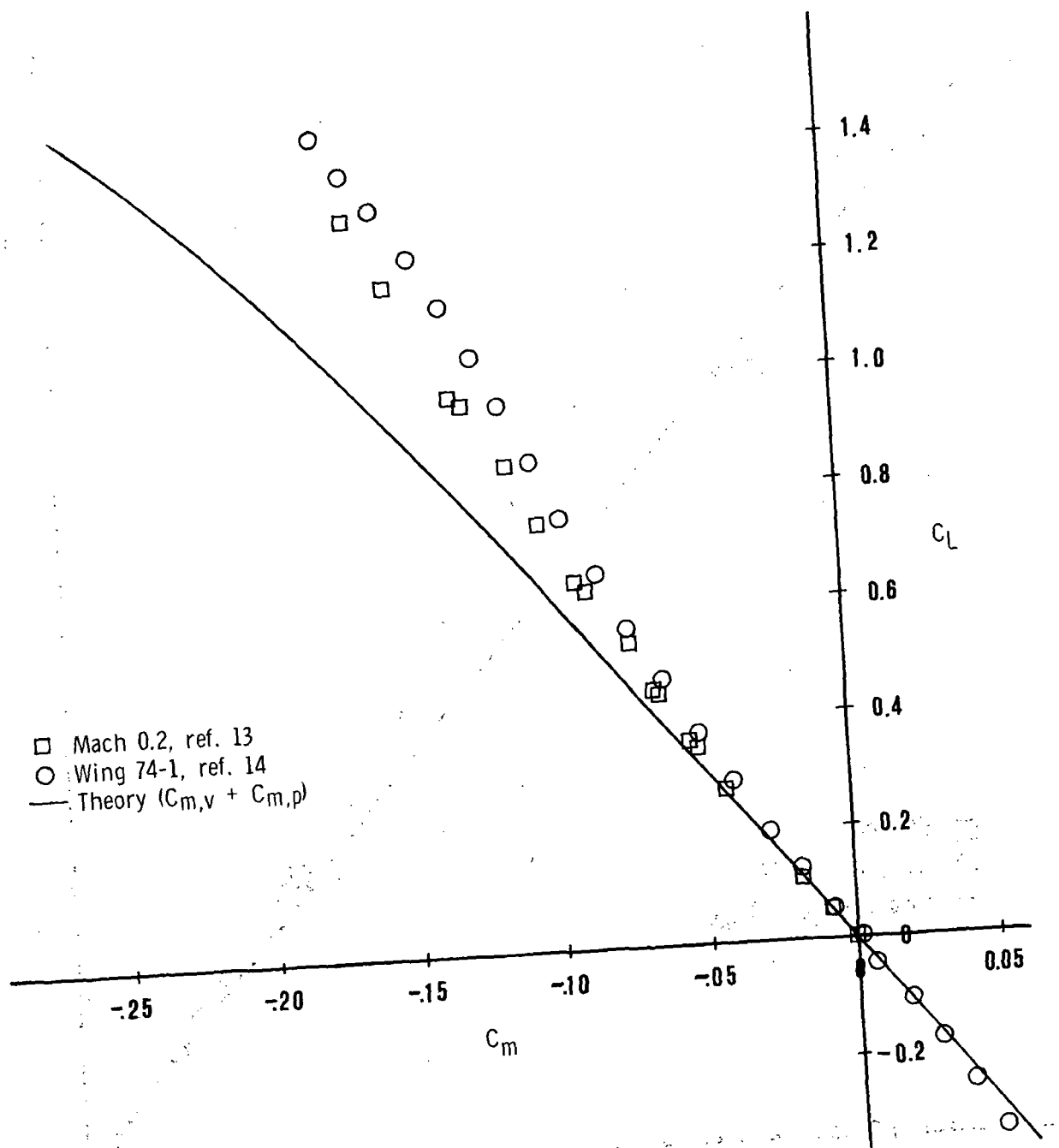


Figure 8.- Variation of C_m as measured and predicted for an $A = 1$ delta wing.





POSTMASTER: If Undeliverable (Section 158
Postal Manual) Do Not Return

"The aeronautical and space activities of the United States shall be conducted so as to contribute . . . to the expansion of human knowledge of phenomena in the atmosphere and space. The Administration shall provide for the widest practicable and appropriate dissemination of information concerning its activities and the results thereof."

—NATIONAL AERONAUTICS AND SPACE ACT OF 1958

NASA SCIENTIFIC AND TECHNICAL PUBLICATIONS

TECHNICAL REPORTS: Scientific and technical information considered important, complete, and a lasting contribution to existing knowledge.

TECHNICAL NOTES: Information less broad in scope but nevertheless of importance as a contribution to existing knowledge.

TECHNICAL MEMORANDUMS: Information receiving limited distribution because of preliminary data, security classification, or other reasons. Also includes conference proceedings with either limited or unlimited distribution.

CONTRACTOR REPORTS: Scientific and technical information generated under a NASA contract or grant and considered an important contribution to existing knowledge.

TECHNICAL TRANSLATIONS: Information published in a foreign language considered to merit NASA distribution in English.

SPECIAL PUBLICATIONS: Information derived from or of value to NASA activities. Publications include final reports of major projects, monographs, data compilations, handbooks, sourcebooks, and special bibliographies.

TECHNOLOGY UTILIZATION PUBLICATIONS: Information on technology used by NASA that may be of particular interest in commercial and other non-aerospace applications. Publications include Tech Briefs, Technology Utilization Reports and Technology Surveys.

Details on the availability of these publications may be obtained from:

SCIENTIFIC AND TECHNICAL INFORMATION OFFICE

NATIONAL AERONAUTICS AND SPACE ADMINISTRATION
Washington, D.C. 20546